Damage detection of bridges considering environmental variability using Hilbert-Huang Transform and Principal Component Analysis

Fernando J. Tenelema[1], Rick M. Delgadillo[1], Joan R. Casas[1]
[1]Department of Civil and Environmental Engineering, Technical University of Catalonia (UPC-BarcelonaTech), Campus Nord, C1 building. Jordi Girona, 1-3, Barcelona, Spain

email: fernando-josue.tenelema@estudiant.upc.edu, rick.milton.delgadillo@upc.edu, joan.ramon.casas@upc.edu

ABSTRACT: Structural Health Monitoring (SHM) systems have been heavily studied worldwide in the past decades. In this field, extensive research has been carried out on vibration-based damage detection (VBDD) techniques in civil structures, especially in bridges. Dynamic responses of a structure manifest a certain degree of sensitivity not only to structural damage but also to any change in operational and environmental conditions, these last factors can mask structural damages. In this sense, the main objective of this paper is to separate structural damage conditions from the changes caused by the environmental effects in a numerical benchmark bridge structure. Temperature is chosen as a global environmental parameter for its significant impact on the waveform, and the Instantaneous Phase Difference (IPD) obtained from an analysis of the Hilbert spectral is studied as the vibration damage feature. Principal Component Analysis (PCA) is applied mainly to the IPD in order to eliminate the environmental influence. Due to the lack of experimental data including the temperature effects, the effectiveness and robustness of the proposed procedure is applied to a numerical benchmark bridge structure generated as part of COST Action TU1402 on quantifying the value of information (VoI) in SHM. The benchmark model consisted of a two-span steel bridge under operational (vehicular traffic) and environmental variability, in which two levels of damage were introduced. The dynamic responses in both healthy and structural damage conditions were obtained from a nonlinear time-history analysis using an open access Python code. As the main concluding remark, the suitability of Hilbert-Huang Transform combined with a PCA-based approach and the instantaneous phase difference to achieve a more robust damage assessment algorithm is verified for the numerical benchmark bridge.

KEY WORDS: Damage detection; Instantaneous Phase Difference (IPD); Hilbert-Huang Transform (HHT); Temperature effect; Principal Component Analysis (PCA).

1 INTRODUCTION

Nowadays, the use of damage identification methods based on structural dynamic parameters, such as natural frequencies, mode shapes, and curvatures are being widely studied [1-3]. However, there is limited information about studies of instantaneous frequencies and phase as a dynamic parameter for damage identification on bridges [4-7]. In addition, for civil structures like bridges, dynamic parameters are always influenced by the environmental variability (e.g. ambient temperature) and operational factors, these conditions may disguise the changes caused by structural damages [8].

In the literature, generally the bridge structures are influenced by the environmental variability, especially the temperature plays a major role in the variation of vibration properties. Yan et al. [9] used a two-step procedure, namely a clustering of the data space into several subregions and the application of local PCA-based damage detection method for the structural health monitoring in a real bridge called Z-24. This method presents two advantages (i) the anomaly of some analyzed days disappears as the non-linearity is taken into account by the local PCA-based method (ii) the novelty index (NI) values increase slightly for damage states with respect to those in the reference state, it means that the local PCA-based method is more sensitive to the damage. Many bridges were studied in the evaluation of model-based methods, which consists in get a correlation between the effects of environmental parameters (such as temperature, humidity) and the dynamic features (such as frequencies, modal shapes). In this context, the effects of environmental conditions on dynamic characteristics can be removed and quantified. For instance, the Z-24 bridge was studied with an AutoRegressive model with eXogenous input [10], a linear filter method was used for the Alamosa Canyon bridge [11], the Ting Kau bridge with a support vector machine algorithm [12]. Besides, others techniques like polynomial regression model [13], polynomial chaos expansion technique [14] and neural network model [15] were used for modelling dynamic parameters under environmental effects.

On the other hand, another approach that is increasing more frequently is the non-model-based methods, which consists of extracting a relevant feature from the structural response, being this feature sensitive to damage but insensitive to operational and environmental factors [16]. Figueiredo et al. [17] used four machine learning algorithms such as factor analysis, Mahalanobis distance, auto-associative neural network and singular value decomposition to separate the damages caused by structural changes from those caused by environmental and operational conditions. Soo et al. [18] proposed a damage detection method based on principal component analysis capable of distinguishing between the effects of structural damages and the damages masked by environmental conditions. This method is tested in a two-dimensional truss structure and in the Z-24 bridge, the results demonstrate the ability to distinguish damage effects from

environmental conditions that affect the damage sensitivity parameters. Hu et al. [19] used the principal component analysis to eliminate environmental effects in a dynamic monitoring system of a footbridge. In addition, a novelty analysis on the residual errors of the PCA model was proposed to provide a statistical indication of damage. Santos et al. [20] proposed four kernel-based algorithms for damage detection under varying environmental and operational conditions, one of which is the nonlinear extension of the linear PCA called kernel principal component analysis (KPCA). The KPCA showed a better performance than the linear PCA and others in an experimental study of three-story frame aluminum structure and shaker. More recently, the linear and nonlinear principal component analysis was used to distinguish between damage effects and environmental factors which affect the damage sensitivity features [17-18]. Hu et al. [21] developed a multiple linear regression (MLR) method to characterize the nonlinear relationship between natural frequencies and temperatures of a prestressed-concrete box girder bridge. The authors demonstrate the ability of the method to identify the gradually realistic deterioration for aging infrastructures using statistical pattern recognition methods.

Recent studies [22-24] showed that the Hilbert-Huang Transform (HHT) and improvements of empirical mode decomposition (EMD) like ICEEMDAN, are widely used methods for analysis of non-linear and non-stationary signals in biomedical and civil engineering, and can be applied for damage identification in bridges [5-6]. The HHT [25] in conjunction with ICEEMDAN [22] method has been used in some scientific and engineering disciplines considering nonstationary and nonlinear physical phenomena. Besides, the researchers have used different sensible dynamic variables for damage identification such as Marginal Hilbert spectrum [4,6,26], phase difference [4,6], instantaneous frequency [5,27], instantaneous amplitude [5,27], a combination of instantaneous frequency and amplitude [27]. Additionally, Dragomiretskiy and Zosso [28] developed the Variational Mode Decomposition (VMD), which is an adaptative and non-recursive decomposition technique. Xin et al. [29] used VMD approach for structural damage identification in nonlinear building model through the decomposition of the dynamic responses. They used as damage sensitive features the instantaneous frequencies obtained from the HT in order to determine the location and severity of the damages. In general, there is little research in bridge applications that use these instantaneous parameters as indicators of damage and even more so including the study of the variation of environmental factors such as temperature that masks structural damage. Therefore, this article presents a new method based on Hilbert-Huang approach and Principal Component Analysis (PCA) in order to remove environmental effects from non-stationary and non-linear signals coming from the traffic effect, and subsequently to identify damages on bridges.

The paper is structured as follows. In section 2, the basic concepts of Hilbert-Huang, Variational Mode Decomposition (VMD) and principal component analysis are introduced. Numerical benchmark model of a bridge is presented in Section 3. In section 4, the proposed approach is applied to this benchmark bridge to verify its effectiveness, two damage cases subject to environmental conditions (changes of temperature) are successfully identified. Finally, Section 5 concludes the paper.

2 FUNDAMENTALS OF METHODS FOR DAMAGE IDENTIFICATION

2.1 Hilbert transform (HT)

In the last decade, the Hilbert transform (HT) [25] has been widely used in many fields of engineering, it has been applied in conjunction with improvements of empirical mode decomposition like ICEEMDAN and VMD in solving static and dynamic, linear and nonlinear problems of damage detection in structures [5,6,27-29].

In this paper, the Hilbert transform and VMD are applied to a given signal of a benchmark numerical bridge to provide enhanced instantaneous phase difference (IPD) information and this IPD will be used for damage detection. Generally speaking, the Hilbert-Huang method aimed for decomposing a non-linear and non-stationary signal into a set of mono-component signals and extracting the corresponding intrinsic mode functions (IMF). Having obtained the IMF components from time history *x(t)*, the second step of the HHT method is implemented by performing the HT to each IMF component $c_n(t)$. The Hilbert transform of a real-valued time domain signal *c(t)* is another real-valued time domain signal, it can be denoted by $\tilde{c}(\mathrm{t})$, such that $z(\mathrm{t}) = \mathrm{c}(\mathrm{t}) + \mathrm{i}\,\tilde{c}(\mathrm{t})$ is an analytic signal. The subscript in $c_n(t)$ is dropped for simplicity, so that the following equation 1 can be written:

$$\tilde{c}(\mathrm{t}) = \int_{-\infty}^{\infty} \frac{c(\mathrm{k})}{\pi(\mathrm{t}-\mathrm{k})}\, dk \tag{1}$$

The VMD technique transforms a mode decomposition problem onto a variational solution problem and was used to overcome certain drawbacks found in the EEMD method. VMD can decompose a multicomponent signal into an ensemble of quasi-orthogonal band-limited IMFs with specific sparsity properties in the spectral domain. Mathematically, the constrained variational problem can be expressed as:

$$\min_{\{u_k\},\{\omega_k\}} \left\{ \sum_k \left\| \partial_t \left[\left(\delta(\mathrm{t}) + \frac{j}{\pi t} \right) * u_k(\mathrm{t}) \right] e^{-j\omega_k t} \right\|_2^2 \right\} \tag{2}$$

$$\text{Subject to } \sum_k u_k = f \tag{3}$$

Where u_k is the *k-th* IMF and ω_k = center pulsation around which the *k-th* IMF is mostly compact, δ is the Dirac distribution and *f* is the original signal. The bandwidth of each mode is estimated by the squared H^1 Gaussian norm of its shifted signal with only positive frequencies. Then, a quadratic penalty and Lagrangian multipliers λ are introduced to transformed into an unconstrained optimization problem. The remaining parameters are explained in detail by [28,30].

On the other hand, Kunwar et al. [4] and Salvino et al. [31] focused attention on the physical meaning of $\theta(t)$ (the instantaneous phase obtained with the HHT) to represent the phase of travelling structural waves of a dynamically

measurable quantity, such as the acceleration, strain, or displacement. $\theta_p(t)$ denotes the instantaneous phase at a particular location *p* on the bridge structure. If a point *o* on the bridge is chosen as a reference point, then the phase function relative to this reference point *o* can be expressed by the following formula:

$$\varphi_p(\mathrm{t}) = \theta_p(\mathrm{t}) - \theta_o(\mathrm{t}) \tag{4}$$

Where φ_p shows the relative phase relationship of a travelling structural wave for a given state of a bridge at the point *p*. Furthermore, due the changes in the dynamic conditions of the bridge that are caused by potential damages, the $\theta_p(t)$ will reflect this behavior as a change on the speed at which energy travels through the bridge. Therefore, in the present study, the instantaneous relative phase $\varphi_p(t)$ is referred to as the Instantaneous Phase Difference (IPD), that demonstrated its good performance for damage identification and localization in many references [4,6,30,31].

2.2 Principal component analysis (PCA)

PCA is a well-known linear method for data analysis, which is used for mapping multidimensional data and as a dimensional reduction tool [32]. In this regard, a large number of interrelated variables can be represented into low-dimensional uncorrelated variables by an orthogonal projection with minimal redundancy, in which the new reduced coordinates are known as principal components. Besides, damage sensitivity features collected from bridge structures subjected to environmental conditions can be processed by PCA to extract the main factors driving the variances in the data set [18]. In the present paper, PCA is used to extract the differences and similarities in the original data set rather than reducing the dimensions of the original data set.

Firstly, *Z* denotes a *nxp* data set of *n* damage sensitivity features collected from *p* observations with $n<p$. In this study, one damage sensitive parameter such as instantaneous phase is chosen as the feature, this damage parameter is represented by *n* and *p* represents the amount of time the instantaneous phase is collected. Mathematically it can be shown as:

$$Z = \begin{bmatrix} X_{1,1} & \cdots & X_{1,\mathrm{p}} \\ \vdots & \ddots & \vdots \\ X_{\mathrm{n},1} & \cdots & X_{\mathrm{n,p}} \end{bmatrix} \tag{5}$$

As mentioned [18], PCA transforms the data set X into a new *mxp* data set *Y* with smaller dimensions which characterizes most of the variances in the original data set. In this regard, a transform matrix *T* is used to relation the *Y* and *X*, which has dimensions *mxn* as shown in equation 6.

$$Y = TX \tag{6}$$

Where *Y* is the score matrix and it represents a new set of data which combines the scores of each observation obtained for the factors affecting the original data set. The factors which represent the environmental effects are called principal components, these damage sensitivity features are affected by damage of structural components. Besides, the first principal components are represented by who present most of the variances in the original data set, and the second component accounts for the second most variance, and so on [18].

T is called loading matrix and its rows correspond to the eigenvectors of the covariance matrix of *X*. The singular value decomposition can be applied to obtain the eigenvectors of the covariance matrix *X*. This relationship can be expressed as

$$\frac{1}{p-1} XX^T = U \frac{\sum^2}{p-1} U^T \tag{7}$$

Where *U* = orthonormal matrix ($UU^T = I$) whose columns represent the eigenvector of the covariance matrix of *X* (hence $T = U^T$), and the summary is obtained by

$$\sum = \begin{bmatrix} \sum_1 & 0 \\ 0 & \sum_2 \end{bmatrix} \tag{8}$$

Where the singular values are represented by $\sum_1 = diag(\sigma_1, \sigma_2, ..., \sigma_m)$ and $\sum_2 = diag(\sigma_{m+1}, \sigma_{m+2}, ..., \sigma_n)$. The $\sum_1$ and $\sum_2$ are organized in descending order $(\sigma_1 \geq \sigma_2 \geq ... \geq \sigma_m \geq \sigma_{m+1} \geq ... \geq \sigma_n \to 0)$. Finally, the damage detection can be obtained considering the analysis of the only first few row of the score matrix (first few principal components in PCA method). Therefore, the number of principal components should be chosen carefully in order to avoid the false detections [18].

3 APLICATION TO THE NUMERICAL BENCHMARK BRIDGE

In this section, a benchmark bridge was studied, which represents the superstructure component of a two-span continuous steel beam bridge. This benchmark numerical model was developed by [33] via open-source Python scripts which are made available through GitHub. This bridge was developed as a part the scientific networking project COST Action TU1402 on Quantifying the Value of SHM.

This numerical model has a total length L = 20m as sketches in Figure 1. The bridge superstructure presents two-span continuous beam with equal span lengths (L_1= L_2=10m). This beam model has a rectangular cross section with constant width b = 0.1m and height h = 0.6m. The material of the beam is low carbon structural steel (Grade S235) and the mechanical properties are Young's modulus E = 215 GPa, Poisson's ratio ν = 0.3 and material density ρ = 7850 kg/m3 at ambient temperature of T = 20ºC. The three supports present 10^6kN/m and 10^{15}kN/m for the horizontal and vertical stiffness respectively. Finally, the study of the finite element analysis, mesh refinement and other considerations are reported in detail in [30]. The bridge is crossed by a punctual load at a specified speed representing the effects of the vehicular traffic. The passage of a vehicle is modeled as a moving load *F* with constant speed *v*, as plotted in Figure 1.

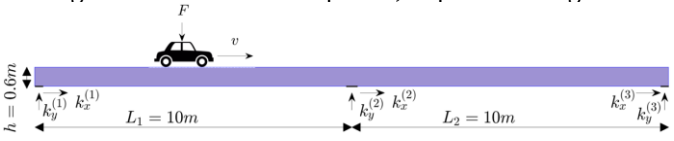

Figure 1. Geometry of the benchmark numerical bridge.

On the other hand, several damage scenarios that represent "cracks" on the beam surface were imposed to the numerical bridge, which are modelled by reducing Young's modulus at the Gauss points on particular finite elements. Furthermore, six sensing points called "sensors" are considered to provide information about the nodal variables in both x (horizontal) and y (vertical) directions. Six damage scenarios grouped in two damage regions are imposed and the sensors (green points) are shown in Figure 1. Their exact location is presented in Table 1.

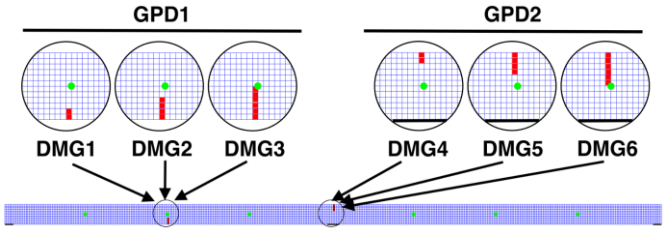

Figure 2. Location of sensors and damage scenarios in benchmark numerical bridge.

Table 1. Location of sensors along the beam.

Sensors	Description	Location along the neutral axis of the beam (y=0.3m)
S-01	at ¼L_1 left-hand	x = 2.5 m-
S-02	at ½L_1 left-hand	x = 5.0 m
S-03	at ¾L_1 left-hand	x = 7.5 m
S-04	at ¾L_2 right-hand	x = 12.5 m
S-05	at ½L_2 right-hand	x = 15.0 m
S-06	at ¼L_2 right-hand	x = 17.5 m

In order to simulate the extent of damage, each damage differs from each other in the number of damaged mesh elements, as presented in Table 2. For example, the damage 1 and 4 involve an area of two damaged elements, the damage 2 and damage 5 consider an area of four damaged elements, and finally the damage 3 and damage 6, a zone of six damaged elements. In addition, the damaged elements have a width of 0.05 m and the height ranges from 0.1 to 0.3 m.

Table 2. Description of damage states performed on the numerical steel beam.

Damage scenarios	Mesh elements	Damage location
Undamaged (UND)	0	
Damaged 1 (DMG1)	2	at ½ L_1 from the left-hand support, starting from the bottommost edge
Damaged 2 (DMG2)	4	
Damaged 3 (DMG3)	6	
Damaged 4 (DMG4)	2	at ½ L_2 from the right-hand support, starting from the uppermost edge
Damaged 5 (DMG5)	4	
Damaged 6 (DMG6)	6	

Additionally, the six damage scenarios are classified in two groups (GPD1 and GPD2) in order to study the influence of damage severity corresponding to the percentage of stiffness reduction (SR). The effects of damage extension are represented by the number of damaged elements. For the group of damage 1 (GPD1), the damage is located at the mid-left span (x=5m). The effects of damage severity are taken into account by reducing the stiffness by 50%, 70% and 90%. While for group of damage 2 (GPD2), the damage extension above the intermediate support was studied, for a 70% of stiffness reduction (SR=70%).

4 RESULTS

The time-varying parameter *instantaneous phase difference* (IPD) is defined as a local measurement recorded by sensors placed in several locations of the bridge, as shown in previous section. Considering a particular point in the bridge, the measurement of accelerations under transient loads may be treated as a local measurement since it represents the forced vibration behavior of this particular point (or mesh node in finite element modelling). Furthermore, this point is different from the vibration behavior at any other analyzed point in the bridge.

The number of the IMFs m considered in the analysis, varies from sensor to sensor. For instance, $m=6$ for sensors S-01, S-03, S-04 and S-06, and $m=5$ for sensors S-02 and S-05. The instantaneous modal parameters were obtained during 2 seconds and an output time-step size of Δt = 0.0025 seconds (equivalent to a sampling frequency of 400 Hz) was selected to obtain the first three bending modes of vibration.

The results for the healthy condition (undamaged) and the damage cases corresponding to GPD1 and GPD2 at temperatures of -10°C, 0°C, 20°C, 40°C are considered in the analysis to take into account the influence of the temperature effects. In addition, three extreme cases at low temperatures around -30°C (blue lines) and other three extreme cases at high temperatures around 70°C (red lines) for the undamaged state were considered to create the baseline. From here on, both the undamaged cases and the damaged scenarios will be represented by the colors as shown in Figure 1.

4.1 Instantaneous phase difference (IPD)

In the whole analysis, the IPD has been calculated taking sensor 01 as the reference sensor. The IPD obtained from each IMF of sensor S-01 for the baseline (red and blue curves) and the other monitored cases at different temperatures (colorful curves) are shown in Figure 1. In particular, the monitored cases are found within the baseline limits. Moreover, the boundary condition effect is present at the end of the study time interval, particularly, in the high-frequency modes (IMF1 and IMF2).

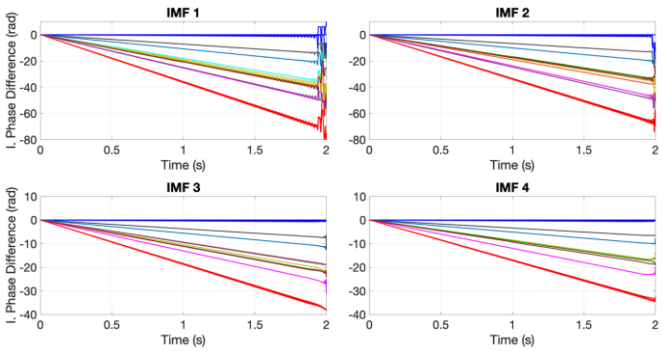

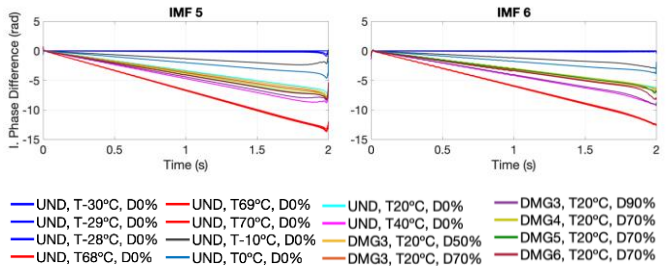

Figure 3. Instantaneous phase difference for different damage scenarios and temperature conditions corresponding to each IMF obtained from sensor S-01.

The six modes (IMFs) shown in Figure 3 are taken into account for the application of PCA using data from 0.1 to 1.5 seconds, which are equivalent to 560-time samples. In order to satisfy the ability for damage detection, the baseline should show a clear separation (gap) between the coldest and hottest limits. Furthermore, if the number of time samples meeting this condition is noted as *S*, then the percentage of these samples with respect the total number of samples studied will be expressed as $P_{gap} = S/560x100$. Considering the first principal component, the percentage of monitored samples lying inside (S_{in}) the temperature limits with respect to *S* can be computed as $P_{in} = S_{in}/S$. Likewise, in the case of the second PC, the percentage of time samples lying outside (S_{out}) the temperature limits with respect to *S* is expressed as $P_{out} = S_{out}/S$.

In this sense, Figure 1 depicts the first two principal components for four undamaged cases at -10ºC, 0ºC, 20ºC and 40ºC (from top to bottom). The monitored values are represented by black dots in all plots. For all cases, the two extreme conditions used as baseline have a clear separation between them, thus only the first component is used for analysis and the others are disregarded. Moreover, in the four cases, the magnitude of the observations in the PC1 is much larger than that in the PC2 for all four undamaged cases since the PC1 indicates nearly 100% of the information of the original data, while the PC2 merely represents any information. In addition, the percentage of gap, P_{gap}, in the PC1 is 100% for the four cases and all the monitored conditions are found inside the limits $P_{in} = 100\%$. Afterwards, with respect to PC1, the evolution of temperature is plotted from the undamaged case at -10ºC to the undamaged case at 40ºC. The monitored cases (black dots) displace from the coldest temperature limit (blue dots) to the hottest temperature limit (red dots) when increasing temperature.

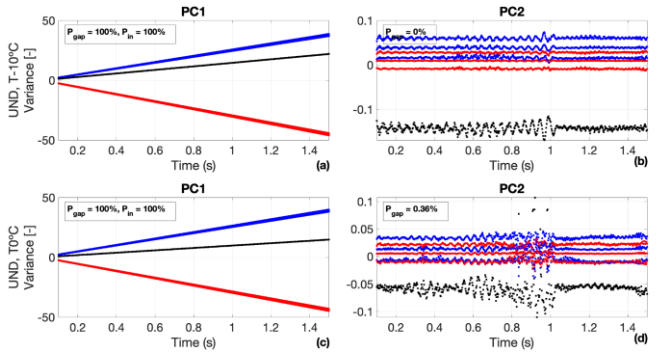

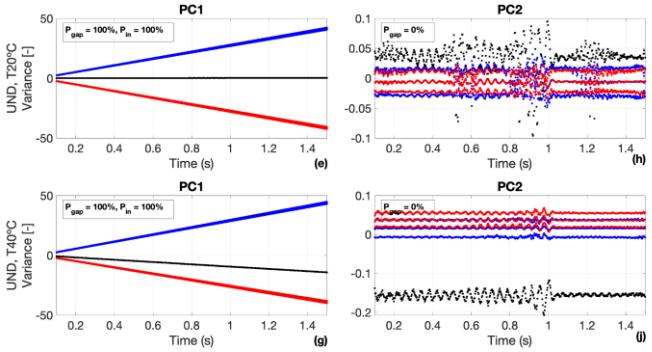

Figure 4. First and second PCs regarding the IPD obtained from sensor S-01 for four undamaged cases, from 0.1 to 1.5 s. and 4 temperature values

Likewise, the T-scores of the principal components was normalized for a better representation considering all damage cases. The T-scores corresponding to the baseline are standardized within 0 and 1, where 0 represents the limit of the highest temperatures (shown as red dots), and 1 represents the upper limit of the lowest temperatures (blue dots). Then, the normalized T-scores corresponding to the monitored cases are computed by a linear interpolation of the normalized T-scores for the baseline. Finally, taking into account the fact that a gap (separation) should exist between the two extreme temperatures conditions, only the monitored cases at each time sample meeting this condition will be shown in the following plots.

Figure 1 gives the first and second principal components for the damaged cases of the GPD1. Figure 1 reflect that all points meet the condition for damage identification purposes in PC1 $(P_{gap}=100\%)$, likewise, all the monitored cases lie inside the temperature limits $(P_{in}=100\%)$. The behavior of the monitored case tends to move to the hottest limit when the severity of damage increase, suggesting a rise in temperature when in fact there is not such a change. Besides, the influence of the highest and lowest-frequency modes in data set when the damage is severe make cause part of the damage to be interpreted as an increase in temperature. On the other hand, Figure 1 depict the damage evolution of the PC2. In this case, P_{gap} increases when the severity of damage grows from 42% to 100%, while all the monitored cases lie outside the baseline limits $(P_{out}=100\%)$ for all cases, giving rise to damage alerts. It should be pointed out that, when damage increases, the monitored cases are no longer dispersed and become more constant over time. This is consequence that the T-scores corresponding to the three extreme cases with close temperature are very similar.

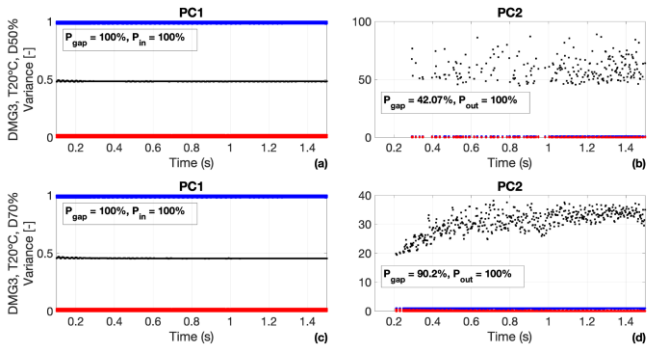

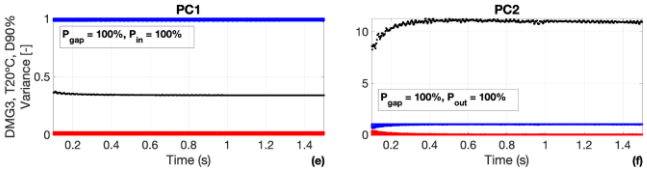

Figure 5. First and second PCs regarding the IPD obtained from sensor S-01 for the damage cases of the GPD1.

In conclusion, it can be noticed that as damage increases, more time samples between 0.2 and 0.8 seconds, approximately, meet the condition for damage detection. Therefore, it may suggest that the structural damage is located within this range, equivalent to 2 to 8 meters.

Figure 1 gives the first and second principal components for the damaged cases of the GPD2. Figure 1 confirm that all the points meet the condition for damage identification purposes in PC1 *(P_{gap}=100%)*, likewise, all the monitored cases lie inside the temperature limits *(P_{in}=100%)*. Thus, the temperature condition is found at the temperature average of the two extreme conditions, which is 20ºC. Figure 1 depict the damage evolution of the PC2. In this case, P_{gap} increases when the severity of damage grows (from 2 to 4 damaged elements), except for the last case in which P_{gap} has been reduced with respect to the other damaged cases. This may be related to the influence of symmetric bending modes over the other. Finally, the percentage of monitored cases lying outside the baseline limits, P_{out}, is always 100% for all cases, giving rise to damage alerts.

Additionally, with respect to the location of damage, a slight variation occurs around 1 second in the PC1 for all damage scenarios, right after the load passes over the damage zone. This may give a rough estimate of the location of damage and this change around 1 second can also be seen in the PC2, where the variance of the monitored cases increases, thus producing two clusters: one from 1 – 1.5 seconds above another from 0.2 to 1 second (Figure 1).

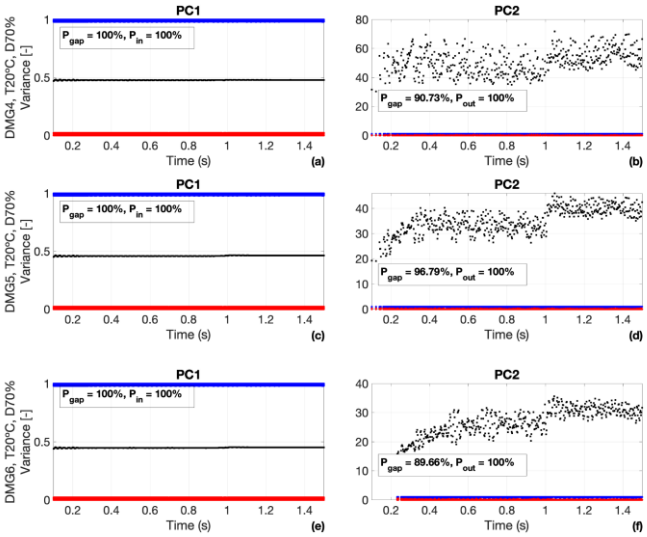

Figure 6. First and second PCs regarding the IPD from sensor S-01 for damage cases of the GPD2, from 0.1 to 1.5 s.

On the other hand, because the overall data set is very large, the results studied in the present investigation are only presented for three sensors. Figure 1 show the instantaneous phase (IPD) for each IMF under temperature variations for both sensor 4 and 6 respectively. The monitored cases are found within the baseline limits and the boundary effects problem is present at the end of the study time interval both for sensor 4 and 6, especially in the high-frequency modes (IMF1 and IMF2).

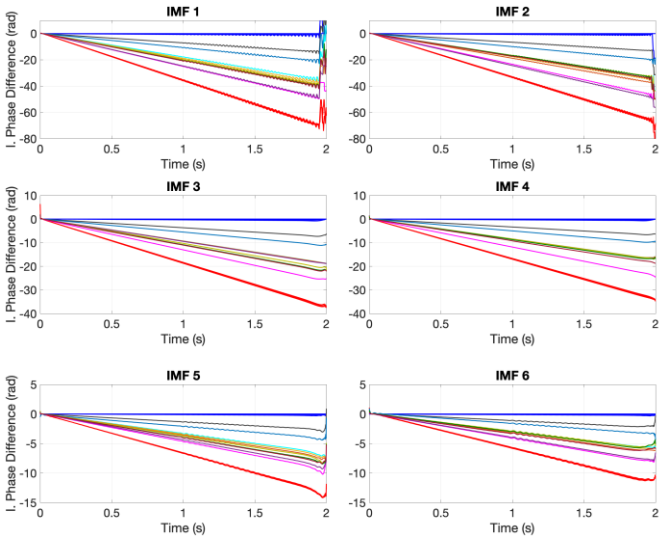

Figure 7. Instantaneous phase difference for the baseline and monitored cases obtained from sensor S-04.

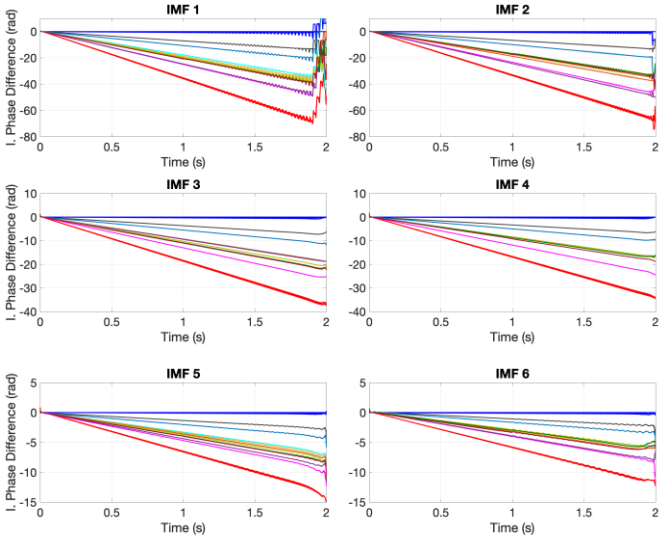

Figure 8. Instantaneous phase difference for the baseline and monitored cases obtained from sensor S-06.

An in-depth study was done for sensors 4 and 6 and the results are plotted in Figures 9 to 12. Figures 9 and 10 show the results for GPD1 and GPD2 in sensor 4 respectively, and the Figures 11 and 12 depict same cases in sensor 6. The results for sensors S-04 and S-06 show that for a low level of damage (SR50%), no damage is detected and for a stiffness reduction of 70%, the number of samples meeting the damage condition increases between 20 to 80 % as in S-01. Furthermore, in the sensors S-04 and S-06 for a SR over 70%, there is more dispersion of the monitored cases from 1 to 1.5

seconds, while from 0.2 to 1 seconds a clear cluster is identified.

In conclusion, the proposed methodology is efficient to distinguish structural damage from temperature effects. Regarding the undamaged cases, the temperature condition of the structure can be estimated without the need of a direct temperature measurement. Regarding the damaged cases, generally when the damage increases, the number of time samples meeting the damage condition increases. Therefore, both the damage severity and the damage extension is reflected in the results.

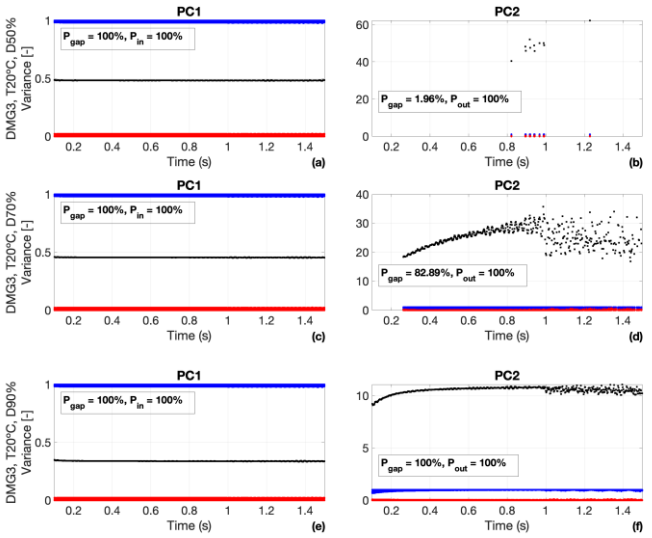

Figure 9. PC1 and PC2 obtained from sensor S-04 corresponding to the GPD1.

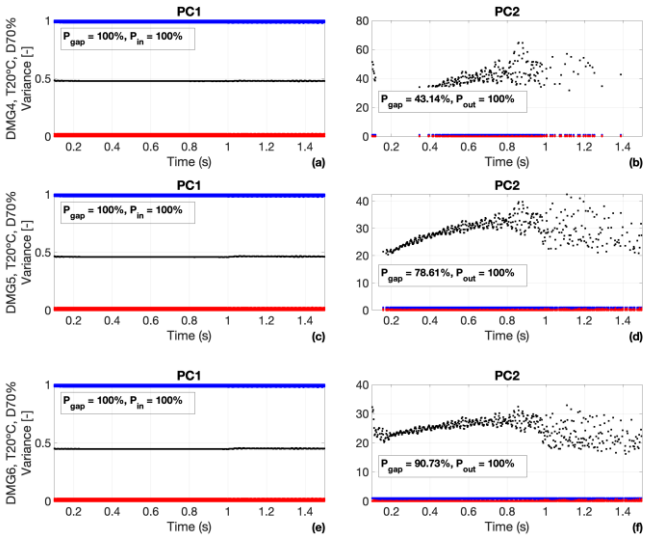

Figure 10. PC1 and PC2 obtained from sensor S-04 corresponding to the GPD2.

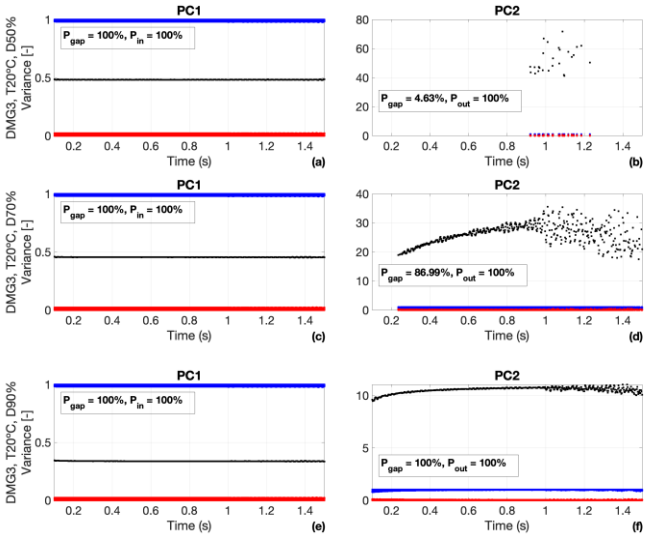

Figure 11. PC1 and PC2 obtained from sensor S-06 corresponding to the GPD1.

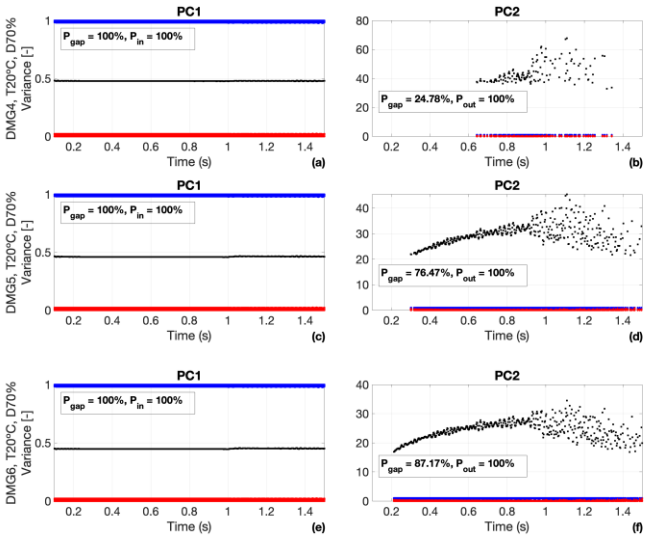

Figure 12. PC1 and PC2 obtained from sensor S-06 corresponding to the GPD2.

5 CONCLUSIONS

The paper demonstrates the potential of the proposed methodology in assessing and monitoring the structural condition of the benchmark numerical bridge under changing operational and environmental conditions. The major advantage of this method is that damages are detected, localized and quantified using bridge response under operational conditions while considering the environmental variability like temperature.

The results presented in this investigation show good performance of the damage-sensitive feature like instantaneous phase difference (IPD). In this sense, this time-varying parameter was obtained using HHT-based method for each intrinsic mode function (IMF) under different temperature conditions. The principal component analysis (PCA) is adopted for data processing, and the first two principal components of each data set was analyzed, and the damage effects were distinguished from the effects of the

environmental variability. The IPD of each IMF linearly decreases along time with no fluctuations, and this damage feature can be a good parameter to separate the temperature effects from structural damages, as well as to detect the severity of damage.

To conclude, this mixed combined method of HHT and PCA not only detect the presence of damage in the bridge, but also quantify the severity or extent of the damage by recognition of patterns in the original data set.

ACKNOWLEDGMENTS

The second author wishes to express their gratitude for the financial support received from PRONABEC Program of Peruvian Ministry of Education with the President of the Republic Scholarship for the great support on his PhD studies. The authors wish to thank the Prof. Eleni Chatzi, ETH Zurich, for their valuable sharing of the entire data from numerical benchmark bridge used in the present research. Authors are indebted to the Secretaria d' Universitats i Recerca de la Generalitat de Catalunya for the funding provided through AGAUR (2017 SGR 1481).

REFERENCES

[1] Chul-Woo Kim. Modal-parameter identification and vibration-based damage detection of a damaged steel truss bridge. Engineering Structures. 122 (2016): 156-173.

[2] OBrien EJ, Malekjafarian A. A mode shape-based damage detection approach using laser measurement from a vehicle crossing a simply supported bridge. Structural Control and Health Monitoring. 2016 Oct;23(10):1273-86.

[3] Liu F, Li H, Yu G, Zhang Y, Wang W, Sun W. New damage-locating method for bridges subjected to a moving load. Journal of Ocean University of China. 2007 Apr 1;6(2):199-204.

[4] Kunwar, A, Jha, R, Whelan, M, & Janoyan, K. Damage detection in an experimental bridge model using Hilbert–Huang transform of transient vibrations. Structural Control and Health Monitoring, 20(1), 2013, 1-15.

[5] Delgadillo RM, Casas JR. SHM of bridges by improved complete ensemble empirical mode decomposition with adaptive noise (ICEEMDAN) and clustering. Enabling Intelligent Life-cycle Health Management for Industry Internet of Things (IIOT). Proceedings of IWSHM. 2019:2111-2118.

[6] Delgadillo RM, Casas JR. Damage detection in a real truss bridge using Hilbert-Huang Transform of transient vibrations. 10th International Conference on Bridge Maintenance, Safety and Management (IABMAS 2020), 11 – 15 April 2021, Sapporo Convention Center, Japan (pp.1-8).

[7] Zhang RR, King R, Olson L, Xu YL. Dynamic response of the Trinity River Relief Bridge to controlled pile damage: modeling and experimental data analysis comparing Fourier and Hilbert–Huang techniques. Journal of Sound and Vibration. 2005 August 6;285(4-5):1049-1070.

[8] Sohn H, Worden K, Farrar CR. Statistical damage classification under changing environmental and operational conditions. Journal of intelligent material systems and structures. 2002 Sep;13(9):561-74.

[9] Yan AM, Kerschen G, De Boe P, Golinval JC. Structural damage diagnosis under varying environmental conditions—part II: local PCA for non-linear cases. Mechanical Systems and Signal Processing. 2005 Jul 1;19(4):865-80.

[10] Peeters B, De Roeck G. One-year monitoring of the Z24-Bridge: environmental effects versus damage events. Earthquake engineering & structural dynamics. 2001 Feb;30(2):149-71.

[11] Sohn H, Dzwonczyk M, Straser EG, Kiremidjian AS, Law KH, Meng T. An experimental study of temperature effect on modal parameters of the Alamosa Canyon Bridge. Earthquake engineering & structural dynamics. 1999 Aug;28(8):879-97.

[12] Ni YQ, Hua XG, Fan KQ, Ko JM. Correlating modal properties with temperature using long-term monitoring data and support vector machine technique. Engineering Structures. 2005 Oct 1;27(12):1762-73.

[13] Ding Y, Li A. Temperature-induced variations of measured modal frequencies of steel box girder for a long-span suspension bridge. International Journal of Steel Structures. 2011 Jun 1;11(2):145-55.

[14] Spiridonakos MD, Chatzi EN, Sudret B. Polynomial chaos expansion models for the monitoring of structures under operational variability. ASCE-ASME Journal of Risk and Uncertainty in Engineering Systems, Part A: Civil Engineering. 2016 Sep 1;2(3):B4016003.

[15] Ni YQ, Zhou HF, Ko JM. Generalization capability of neural network models for temperature-frequency correlation using monitoring data. Journal of structural engineering. 2009 Oct;135(10):1290-300.

[16] Huang JZ, Li DS, Li HN, Song GB, Liang Y. Damage identification of a large cable-stayed bridge with novel cointegrated Kalman filter method under changing environments. Structural Control and Health Monitoring. 2018 May;25(5):e2152.

[17] Figueiredo E, Park G, Farrar CR, Worden K, Figueiras J. Machine learning algorithms for damage detection under operational and environmental variability. Structural Health Monitoring. 2011 Nov;10(6):559-72.

[18] Soo Lon Wah W, Chen YT, Roberts GW, Elamin A. Separating damage from environmental effects affecting civil structures for near real-time damage detection. Structural Health Monitoring. 2018 Jul;17(4):850-68.

[19] Hu WH, Moutinho C, Caetano E, Magalhães F, Cunha A. Continuous dynamic monitoring of a lively footbridge for serviceability assessment and damage detection. Mechanical Systems and Signal Processing. 2012 Nov 1;33:38-55.

[20] Santos A, Figueiredo E, Silva MF, Sales CS, Costa JC. Machine learning algorithms for damage detection: Kernel-based approaches. Journal of Sound and Vibration. 2016 Feb 17;363:584-99.

[21] Hu WH, Tang DH, Teng J, Said S, Rohrmann R. Structural health monitoring of a prestressed concrete bridge based on statistical pattern recognition of continuous dynamic measurements over 14 years. Sensors. 2018 Dec;18(12):4117.

[22] Colominas MA, Schlotthauer G, Torres ME. Improved complete ensemble EMD: A suitable tool for biomedical signal processing. Biomedical Signal Processing and Control. 2014 Nov 1;14:19-29.

[23] Zhu L, Malekjafarian A. On the Use of Ensemble Empirical Mode Decomposition for the Identification of Bridge Frequency from the Responses Measured in a Passing Vehicle. Infrastructures. 2019 June;4(2):32.

[24] Khan I, Shan D, Li Q, Jie H. Continuous modal parameter identification of cable-stayed bridges based on a novel improved ensemble empirical mode decomposition. Structure and Infrastructure Engineering. 2018 Feb 1;14(2):177-191.

[25] Huang NE, Shen Z, Long SR, Wu MC, Shih HH, Zheng Q, Yen NC, Tung CC, Liu HH. The empirical mode decomposition and the Hilbert spectrum for nonlinear and non-stationary time series analysis. Proceedings of the Royal Society of London. Series A: mathematical, physical and engineering sciences. 1998 Mar 8;454(1971):903-95.

[26] Wu SP, Qin GJ, Zou JH, Sun H. Structure health monitoring based on HHT of vibration response from unknown excitation. In Proceedings of the 8th International Symposium on Test and Measurement 2009 (Vol. 1, p. 6).

[27] Delgadillo RM, Casas JR. Non-modal vibration-based methods for bridge damage identification. Structure and Infrastructure Engineering. 1-22, 2019.

[28] Dragomiretskiy K, Zosso D. Variational mode decomposition. IEEE transactions on signal processing. 2013 Nov 5;62(3):531-44.

[29] Xin Y, Li J, Hao H. Damage Detection in Initially Nonlinear Structures Based on Variational Mode Decomposition. International Journal of Structural Stability and Dynamics. 2020 Sep 13;20(10):2042009.

[30] Tenelema, F. Bridge Damage Identification under operational and environmental variability. Master Thesis, Technical university of Catalonia (BarcelonaTeach). 2020.

[31] Salvino LW, Pines DJ, Todd M, Nichols JM. EMD and instantaneous phase detection of structural damage. In Hilbert–Huang Transform and Its Applications 2014 (pp. 301-336).

[32] Jolliffe, I. Principal Component Analysis. 2nd. ed. New York, United States: Springer-Verlag, 2002.

[33] Tatsis, K., Chatzi, E., A numerical benchmark for system identification under operational and environmental variability, IOMAC-2019, 8th International Operational Modal Analysis Conference, May 12th – 14th 2019, Copenhagen (2019).